Biochemical and Biophysical Research Communications 458 (2015) 687–692

Contents lists available at ScienceDirect

Biochemical and Biophysical Research Communications

journal homepage: www.elsevier.com/locate/ybbrc

Bovine leukemia virus nucleocapsid protein is an efficient nucleic acid chaperone

Dominic F. Qualley*, Victoria L. Sokolove, James L. Ross

Department of Chemistry and Biochemistry, Berry College, Mt. Berry, GA, USA

ARTICLE INFO

Article history:
Received 13 January 2015
Available online 14 February 2015

Keywords:
Nucleocapsid
Bovine leukemia virus
Nucleic acid chaperone
Reverse transcription
Annealing kinetics

ABSTRACT

Nucleocapsid proteins (NCs) direct the rearrangement of nucleic acids to form the most thermodynamically stable structure, and facilitate many steps throughout the life cycle of retroviruses. NCs bind strongly to nucleic acids (NAs) and promote NA aggregation by virtue of their cationic nature; they also destabilize the NA duplex via highly structured zinc-binding motifs. Thus, they are considered to be NA chaperones. While most retroviral NCs are structurally similar, differences are observed both within and between retroviral genera. In this work, we compare the NA binding and chaperone activity of bovine leukemia virus (BLV) NC to that of two other retroviral NCs: human immunodeficiency virus type 1 (HIV-1) NC, which is structurally similar to BLV NC but from a different retrovirus genus, and human T-cell leukemia virus type 1 (HTLV-1) NC, which possesses several key structural differences from BLV NC but is from the same genus. Our data show that BLV and HIV-1 NCs bind to NAs with stronger affinity in relation to HTLV-1 NC, and that they also accelerate the annealing of complementary stem-loop structures to a greater extent. Analysis of kinetic parameters derived from the annealing data suggests that while all three NCs stimulate annealing by a two-step mechanism as previously reported, the relative contributions of each step to the overall annealing equilibrium are conserved between BLV and HIV-1 NCs but are different for HTLV-1 NC. It is concluded that while BLV and HTLV-1 belong to the same genus of retroviruses, processes that rely on NC may not be directly comparable.

1. Introduction

In retroviruses, the nucleocapsid protein (NC) plays an important role in the viral life cycle as a nucleic acid (NA) chaperone [1]. A nucleic acid chaperone can be defined as a protein that facilitates the rearrangement of nucleic acids into their most thermodynamically stable state. Retroviral NCs are able to perform this task via several discrete mechanisms: NA aggregation, duplex destabilization, and fast NA binding kinetics. During replication, there are a number of processes that require NC's chaperone activity including reverse transcription, integration, and genome dimerization (for recent reviews see Refs. [2,3]). For example, the minus-strand transfer step of reverse transcription requires the transformation of two stable stem-loop structures into a DNA-RNA duplex, maximizing the number of base pairing interactions. Many retroviral NCs share structural homology; they are typically small, basic proteins with 1–2 zinc fingers that each contain a Zn^{2+}-binding motif where three Cys residues and a His residue coordinate a zinc atom. Human immunodeficiency virus type 1 (HIV-1) NC is considered to be the prototypical retroviral NC; it is a 55-residue polypeptide with two Zn fingers and a calculated isoelectric point of 9.86 (Fig. 1). The highly basic nature of HIV-1 NC stems primarily from its α-helical N-terminal domain, and is the driving force behind NC's strong NA aggregation activity [4-7]. The Zn fingers each contain one or two aromatic residues that can interact with nucleobases via stacking interactions, and have been shown to promote duplex destabilization [8-14]. However, prominent structural differences exist between NCs of different retroviruses, and often produce differences in function. For example, the NC from human T-cell leukemia virus type 1 (HTLV-1) possesses an acidic C-terminal domain (CTD); as a result, the overall charge of this NC at physiological pH is virtually neutral (calculated pI = 7.23). Functionally, HTLV-1 NC is a poor NA chaperone compared to HIV-1 NC; the *in vitro* annealing of an RNA hairpin to a complimentary DNA hairpin is much slower, likely a reflection of HTLV-1 NC's weak

* Corresponding author. 2277 Martha Berry Hwy NW, P.O. Box 495016, Mt. Berry, GA 30149-5016, USA.
E-mail address: dqualley@berry.edu (D.F. Qualley).

http://dx.doi.org/10.1016/j.bbrc.2015.02.025
0006-291X/

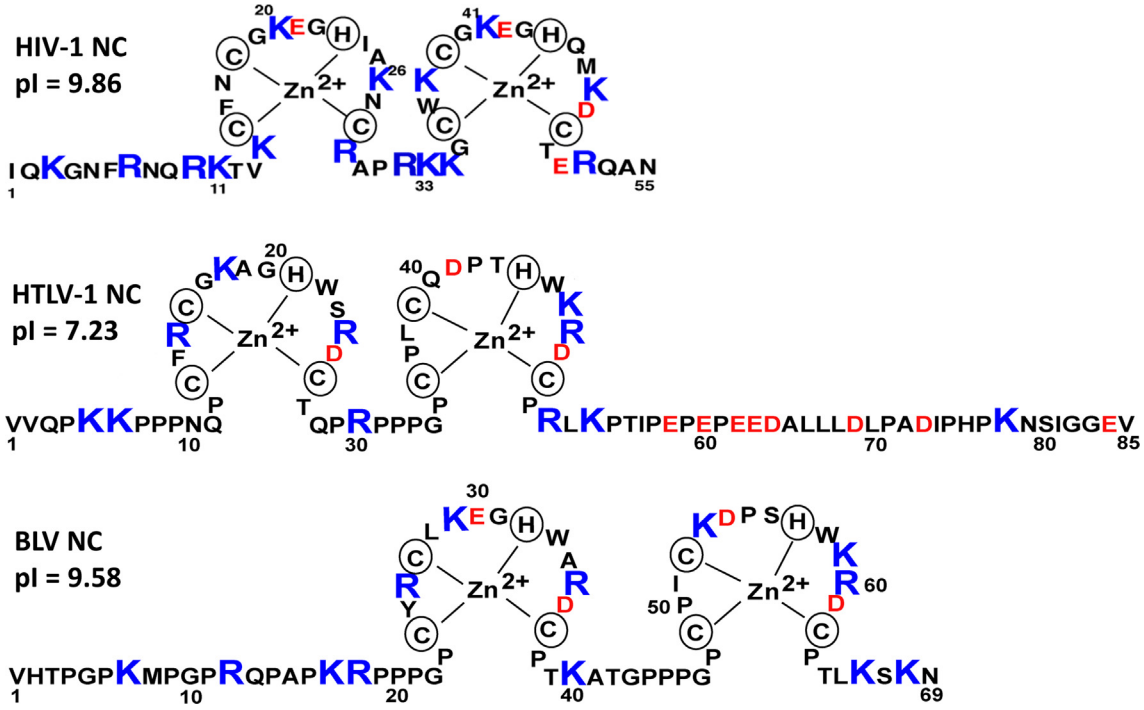

Fig. 1. Primary structure of HIV-1, HTLV-1, and BLV NCs. Acidic residues are in red, basic residues are in blue, and zinc-binding residues have been circled. Isoelectric points were calculated based upon amino acid sequence.

NA aggregation and slow dissociation kinetics [15,16]. Interestingly, HTLV-1 NC facilitates NA duplex destabilization at least as well as HIV-1 NC, lending further support to the hypothesis that destabilization activity is controlled primarily by the Zn finger structures [17]. The CTD of HTLV-1 NC was conclusively shown to be responsible for its diminished NA chaperone activity, as deletion of the CTD improved HTLV-1 NC's NA binding and aggregation activity and resulted in a faster NA dissociation rate [16].

HIV-1 and HTLV-1 belong to different retroviral genera (lentivirus and deltaretrovirus, respectively) so it is reasonable to expect a degree of variability in structure and function between homologous proteins of each virus. Accordingly, retroviral NCs from within the same genus are often similar to one another in this regard. The NC protein from feline immunodeficiency virus (FIV), a lentivirus closely related to HIV-1, promotes efficient annealing and strong NA aggregation due in large part to its highly basic character (pI = 10.56) [18]. A notable exception is found in the deltaretroviruses; although bovine leukemia virus (BLV) is closely related to HTLV-1, its NC is structurally much more similar to HIV-1 NC in that it is basic (pI = 9.58) and it lacks the acidic CTD found in HTLV-1 NC (Fig. 1). A previous study compared the binding affinities of HIV-1, HTLV-1, SIV, and BLV NCs, and found that BLV NC bound more strongly to homopolymeric deoxyribonucleotides than HTLV-1 NC but more weakly than SIV or HIV-1 NCs [19]. BLV NC also has a smaller occluded binding site size (~4 nucleotides) compared to that of HTLV-1 NC (~8 nucleotides), and exhibits a different base preference [19,20].

The understanding of BLV replication and pathogenesis is important for several reasons. As a member of the deltaretrovirus genus, BLV has been proposed as an animal model to develop treatments for HTLV-1 infection in humans [21-24]. Thus, comparative study of these two viruses is needed to determine the applicability of results from BLV experiments to HTLV-1, and vice versa. BLV is also an agriculturally significant pathogen that is prevalent in dairy herds throughout the United States; it infects and causes illness in domestic cattle, and results in diminished milk production [25,26]. Finally, recent evidence suggests that BLV exists in human breast tissue, and may be able to replicate [27,28]. It is unknown how human infection by BLV occurs or if it is pathologically relevant, but better understanding of the molecular mechanisms underlying BLV infection could potentially be of value to public health in the future.

In this study, we compare the NA chaperone activity of BLV NC to HIV-1 NC and HTLV-1 NC with a Förster resonance energy transfer (FRET)-based annealing assay, and show that BLV NC is a much more efficient NA chaperone than the NC from the closely related HTLV-1. Results from NA binding assays are also presented, and show that BLV NC binds efficiently to both a single-stranded DNA (ssDNA) oligonucleotide and a short RNA hairpin derived from the putative BLV packaging signal.

2. Materials and methods

2.1. NA and protein preparation

PCR primers and mini-TAR RNA were purchased from Integrated DNA Technologies (IDT; Coralville, IA) and used without further purification. DNA20 (5' – CTTCTTTGGGAGTGAATTAG – 3′) and SL1 RNA (5' - UAUGGGAAAUUCCCCCUCCUAU – 3′) were also purchased from IDT but were labeled with AlexaFluor488 at the 5′ end, and were purified by nuclease-free HPLC before being shipped. The dual-labeled mini-TAR DNA used for FRET experiments was purchased from Eurofins MWG Operon (Huntsville, AL) and HPLC-purified prior to shipping. This FRET oligomer was labeled with AlexaFluor488 followed by a 6-carbon linker at the 5′ end, and DABCYL at the 3' end.

HIV-1 and HTLV-1 NCs were gifts from Dr. Robert Gorelick (SAIC-Frederick, Inc.). The gene encoding BLV NC was PCR-amplified from a BLV proviral plasmid (a gift from Dr. Kathleen Boris-Lawrie, Department of Veterinary Biosciences, The Ohio State University) and ligated into pET32a (EMD Millipore, Billerica, MA) using standard molecular biology protocols. BLV NC was expressed as a

thioredoxin fusion protein; culture growth and protein expression were performed essentially as described previously [29]. Trx-BLV NC was purified from frozen cell pellets using Ni^{2+}-affinity chromatography. To obtain authentic BLV NC, the fusion protein was treated with TEV protease to cleave the Trx tag, and mature BLV NC was purified using reverse-phase HPLC. Full details of BLV NC cloning and purification are provided in the Supplementary Materials.

2.2. Fluorescence anisotropy (FA) assays

Equilibrium binding of NC proteins to a 20-mer ssDNA (DNA20) and a 22-nucleotide hairpin RNA derived from the BLV packaging signal [30] was measured using FA. Varying concentrations of NC protein were combined with 20 nM of fluorescently-labeled NA in FA buffer (20 mM HEPES, 50 mM NaCl, 5 mM β-mercaptoethanol, 0.1 mM tris(2-carboxyethyl) phosphine hydrochloride, 1 μM $Zn(OAc)_2$, pH 7.5 in diethylpyrocarbonate (DEPC) – treated water). The samples were incubated at room temperature in the dark for 30 min before measuring fluorescence intensities using a Varian Cary Eclipse Fluorescence Spectrophotometer equipped with a manual polarizer accessory. Samples were excited with vertically polarized light at 490 nm, and emission of light parallel (I_{VV}) and perpendicular (I_{VH}) to the excitation axes was measured at 515 nm. The fluorescence anisotropy (A) for each sample was calculated by:

$$A = (I_{VV} - I_{VH})/(I_{VV}+2I_{VH}) \quad (1)$$

and is a measure of the difference in intensity of light parallel versus perpendicular divided by the total intensity. The apparent dissociation constant (K_d) was determined by fitting A as a function of protein concentration (C) to the following equation:

$$A(C) = [A_F + \Theta\cdot(A_B R - A_F)]/[\Theta\cdot(R-1)+1] \quad (2)$$

where

$$\Theta = \left(D + P + K_d - \left((D + P + K_d)^2 - 4DP\right)^{1/2}\right)/2D$$

is the fraction of oligonucleotides bound, D is the oligonucleotide strand concentration, A_B and A_F are the anisotropy values of the fully bound and free oligonucleotides, respectively. R is the ratio of the fluorescence intensity of saturated bound oligonucleotide relative to free oligonucleotide, which accounts for changes in fluorescence intensity upon NC binding assuming a 1:1 oligomer–protein interaction [15]. Non-linear curve fitting was performed using Microcal Origin software, where data from at least three independent trials were globally fit using the Levenberg–Marquardt algorithm.

2.3. FRET-based annealing assays

The mini-TAR nucleic acids were folded into hairpin structures in 15 μL volumes consisting of 20 mM HEPES pH 7.5, 100 mM NaCl, and 15 μM mini-TAR RNA or 0.5 μM dual-labeled mini-TAR DNA, prepared in DEPC H_2O. Each sample was incubated at 80 °C for 2 min followed by 60 °C for 2 min, then $MgCl_2$ was added to final concentration of 10 mM and the sample was stored on ice for at least 30 min. The annealing reactions were prepared as 100 μL volumes in DEPC H_2O and contained 20 mM HEPES pH 7.5, 20 mM NaCl, 300 nM mini-TAR RNA, 10 nM dual-labeled mini-TAR DNA, and 420 nM NC. All components except for NC were combined in a quartz fluorescence cell and allowed to incubate at 30 °C for 15 min. Data collection was performed using the same excitation and emission wavelengths as described above using a temperature-controlled multicell holder accessory set to 30 °C. Intensity readings were taken every minute; NC was added to the cell immediately after the first reading was taken and mixed thoroughly by pipetting. The volume of NC added was as small as possible (<1 μL) to minimize dilution effects upon intensity. To derive kinetic parameters for the annealing reactions, intensity data (I) as a function of time (t) were fit to a double-exponential function:

$$I(t) = I_0 + \left(I_e\left(1 - f e_f^{-kt} - (1-f)e_s^{-kt}\right)\right) \quad (3)$$

where I_0 is the initial intensity, I_e is the equilibrium intensity, f is the fraction of annealing that occurs due to the fast component of the annealing reaction, k_f is the rate constant for the fast component, and k_s is the rate constant for the slow component.

3. Results

3.1. Equilibrium binding experiments

To compare binding affinities of BLV NC, HIV-1 NC, and HTLV-1 NC to biologically relevant NAs, we used FA assays with purified NC and two different fluorescently-labeled NA constructs: DNA20 and SL1 RNA. DNA20 is a construct that has been used previously in several binding studies involving Gag-derived proteins [15,16,29], so while it is not a biologically important sequence in BLV, use of this sequence allows for direct comparison to previously published results. SL1 RNA is a hairpin that is derived directly from a sequence of the BLV genome that has been implicated in packaging of genomic RNA into virions [30]; since the NC domain of Gag is suspected to play a major role in genome encapsidation, this RNA construct is clearly significant to the viral life cycle [31]. Apparent dissociation constants support previous results [19] showing that HIV-1 NC binds with the strongest affinity to NA and HTLV-1 NC the weakest, with BLV NC in the middle (Table 1). For all three NCs, stronger binding occurred to the ssDNA construct over the RNA hairpin. Interestingly, BLV NC did not seem to bind specifically to its SL1 sequence, as the binding affinity is shown to decrease more than threefold compared to the ssDNA. In contrast, HIV-1 NC's affinity for SL1 decreased twofold compared to DNA20.

3.2. FRET-based annealing assays

Overall chaperone activity of the three NC proteins was measured using a FRET-based assay (Fig. 2). When the mini-TAR DNA exists as a hairpin, the fluorophore on the 5′ end is in close proximity to the quencher on the 3' end. As annealing occurs, the DNA is transformed from a hairpin to an extended duplex and fluorescence intensity increases. In this manner, annealing can be measured in real time. Annealing kinetics were best described by a double-exponential function, suggesting a two-step process. These assays were performed at NC concentrations low enough that aggregation would be prevented. Although saturating concentrations

Table 1
Equilibrium dissociation constants for retroviral NC binding to fluorescently labeled oligonucleotides. Values represent a global fit of data from at least three independent trials to Eq. (2).

NC	NA	K_d (nM)
BLV	DNA20	41.05 ± 9.03
	SL1	151.62 ± 30.27
HIV-1	DNA20	25.97 ± 3.78
	SL1	53.54 ± 10.58
HTLV-1	DNA20	428.02 ± 125.05
	SL1	9528.07 ± 4666.5

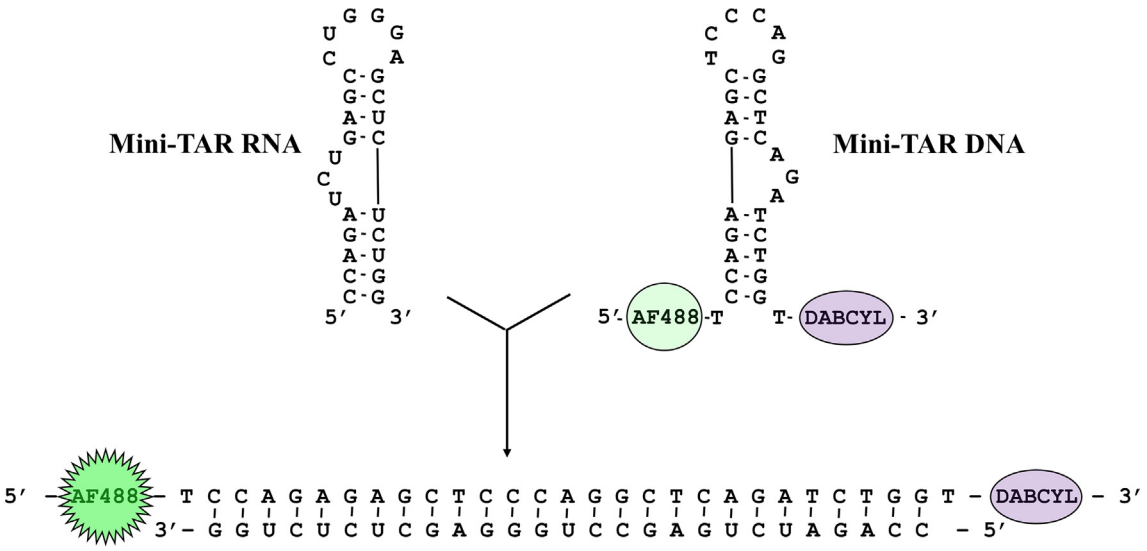

Fig. 2. Reaction scheme of the FRET-based annealing assay used in this study. When mini-TAR DNA exists in a hairpin conformation, the nearby DABCYL quenches the fluorescence signal produced by the AlexaFluor488 (AF488) fluorophore. As annealing of mini-TAR DNA to mini-TAR RNA proceeds, the signal intensity increases, indicating conversion from the hairpin conformation to an extended duplex.

of NC are ideal for measuring annealing kinetics [32], this was not possible using our assay since higher [NC] produced a quick rise in fluorescence intensity as the extended duplex was formed followed by a gradual drop as intermolecular quenching occurred (data not shown). Therefore, instead of using the minimum concentration of each NC required to produce saturation, we used the same concentration for each NC, which still allows direct comparison.

By examining the annealing curves, a striking difference is noted between BLV and HTLV-1 NCs, both deltaretroviruses, as BLV NC accelerates annealing to a much greater extent than HTLV-1 NC (Fig. 3). In contrast, annealing promoted by BLV NC proceeds along the same course as observed for HIV-1 NC, diverging after about 7 min when the annealing reaction is near equilibrium. Upon fitting the fluorescence intensities as a function of time to Eq. (3), we were able to derive several parameters that describe the kinetics of the annealing process (Table 2). The fraction of annealing due to the fast component (f) is similar between HIV-1 and BLV NCs, while this value is much lower for HTLV-1 NC. For the rate constants k_f and k_s, the largest values were for HIV-1 NC and the smallest for HTLV-1 NC, with one exception. In the case of k_f, HTLV-1 NC had the largest rate constant of the three.

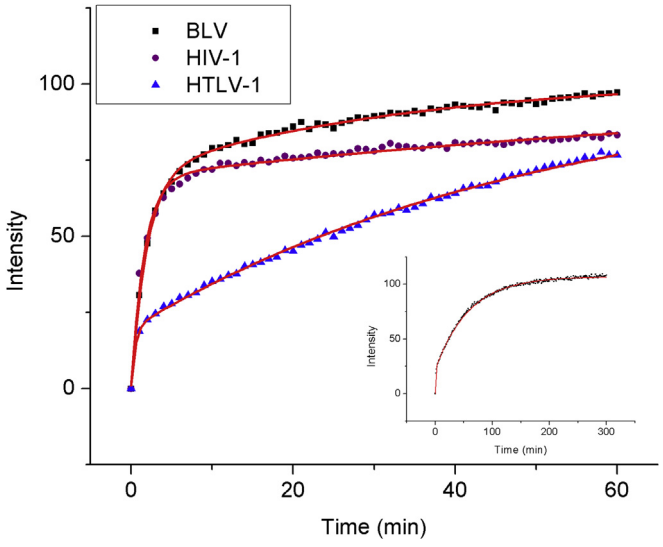

Fig. 3. NC-facilitated annealing of mini-TAR RNA and DNA. Annealing was performed at 30 °C in the presence of 10 nM dual-labeled mini-TAR DNA, 300 nM mini-TAR RNA, and 420 nM NC. Lines represent fits of the data points to Eq. (3). The inset shows annealing with HTLV-1 NC on a longer time scale.

4. Discussion

Our FA results show that BLV NC binds to NA with an affinity between that of HIV-1 NC and HTLV-1 NC. The most directly relevant study tested BLV NC binding to homooctameric oligonucleotides (dG_8, dC_8, dT_8, dA_8) and reported a range of binding affinities between 7 nM (dG_8) to 833 nM (dA_8) [19]. The calculated K_ds from our binding experiments to other NAs fall within this range. In the cited study, BLV NC binding affinities were much closer to those measured for HTLV-1 NC rather than HIV-1 NC, whereas the apparent dissociation constants from our experiments show that BLV NC is closer to HIV-1 NC. It is noteworthy that binding was stronger to the ssDNA than to the RNA hairpin SL1 (predicted to contain 6 base pairs and loop of 9 nucleotides [29]). A strong preference for binding to single-stranded over double-stranded NAs often suggests strong helix destabilization activity [33]. Since the sequences used for our two constructs differ from one another,

Table 2
Kinetic parameters of the mini-TAR annealing reactions. Values were obtained by fitting the data in Fig. 2 to Eq. (3).

NC	I_{eq}	f	k_f (min^{-1})	k_s (min^{-1})
BLV	99.5 ± 1.1	0.69 ± 0.006	0.526 ± 0.017	0.035 ± 0.003
HIV-1	81.8 ± 0.95	0.742 ± 0.010	0.756 ± 0.031	0.061 ± 0.007
HTLV-1	107.2 ± 1.0	0.202 ± 0.008	1.550 ± 0.216	0.017 ± 0.001

it was not possible to calculate the free energy of destabilization as was done previously for HIV-1 NC and HTLV-1 NC [15]. Nonetheless, comparing the relative magnitudes of the K_ds can give an estimate of destabilization produced by each NC. Our data show a ~4-fold decrease in affinity for the double-stranded SL1 for BLV NC, compared to a ~2-fold and a ~22-fold decrease for HIV-1 and HTLV-1 NCs, respectively. This comparison is in line with data showing that HTLV-1 NC is an efficient duplex destabilizer, even more so than HIV-1 NC [16,17].

Next, we examined the ability of each NC to promote the annealing of two complimentary stem-loops. The mini-TAR DNA and RNA are derived from the transactivation response element (TAR) region of the HIV-1 genome, and their annealing into an extended duplex comprises the minus-strand transfer step of reverse transcription [32]. Since the analogous sequence in BLV (if one exists) has not been identified, the mini-TAR system was selected for this assay, where the annealing pathway in the presence and absence of HIV-1 NC has been elucidated in detail [34]. Our assay is insensitive to the formation of a kissing loop complex, and several different annealing pathways initiated at the stem ends are possible, so it is impossible to differentiate between specific mechanisms from our data. However, the values of f and k_s are strongly correlated with the ability of NC to bind to and aggregate NAs, and in this regard, BLV NC is much more similar to HIV-1 NC. It is also worthwhile to mention that fast dissociation kinetics are important for efficient chaperone activity; while its dissociation rate has not been directly measured, the data presented here supports the hypothesis that BLV NC quickly binds to and dissociates from NAs, akin to HIV-1 NC.

Taken together, our results show that despite the close phylogenetic relationship between BLV and HTLV-1, their NC proteins are structurally and functionally different. The significance of these differences to the viral replication process is unknown, but illustrates that proteins from retroviruses representing separate genera may operate in a manner more similar to each other than to analogous proteins from retroviruses within the same genus. Future work to identify the sequences relevant for minus-strand transfer in BLV and HTLV-1 will enable measurement of chaperone activity within those more specific contexts.

Conflict of interest

The authors declare that there are no conflicts of interest.

Acknowledgments

The authors would like to thank Dr. Robert Gorelick for the gift of recombinant HIV-1 and HTLV-1 NC proteins, Dr. Kathleen Boris-Lawrie for the gift of the pKB426 plasmid, and Dr. Ioulia Rouzina for helpful discussions. We are also grateful for support by Berry College in the form of a Faculty Development Grant (to D.F.Q.), a Synovus Scholarship (to V.L.S.), and a Richards Scholarship (to J.L.R.).

Transparency document

Transparency document related to this article can be found online at http://dx.doi.org/10.1016/j.bbrc.2015.02.025.

Appendix A. Supplementary data

Supplementary data related to this article can be found at http://dx.doi.org/10.1016/j.bbrc.2015.02.025.

References

[1] L. Rajkowitsch, D. Chen, S. Stampfl, K. Semrad, C. Waldsich, O. Mayer, M.F. Jantsch, R. Konrat, U. Blasi, R. Schroeder, RNA chaperones, RNA annealers and RNA helicases, RNA Biol. 4 (2007) 118–130.
[2] J.L. Darlix, J. Godet, R. Ivanyi-Nagy, P. Fosse, O. Mauffret, Y. Mely, Flexible nature and specific functions of the HIV-1 nucleocapsid protein, J. Mol. Biol. 410 (2011) 565–581.
[3] J.G. Levin, M. Mitra, A. Mascarenhas, K. Musier-Forsyth, Role of HIV-1 nucleocapsid protein in HIV-1 reverse transcription, RNA Biol. 7 (2010) 754–774.
[4] M. Mitra, W. Wang, M.N. Vo, I. Rouzina, G. Barany, K. Musier-Forsyth, The N-terminal zinc finger and flanking basic domains represent the minimal region of the human immunodeficiency virus type-1 nucleocapsid protein for targeting chaperone function, Biochemistry 52 (2013) 8226–8236.
[5] H. Wu, M. Mitra, M.N. Naufer, M.J. McCauley, R.J. Gorelick, I. Rouzina, K. Musier-Forsyth, M.C. Williams, Differential contribution of basic residues to HIV-1 nucleocapsid protein's nucleic acid chaperone function and retroviral replication, Nucleic Acids Res. 42 (2014) 2525–2537.
[6] E. Le Cam, D. Coulaud, E. Delain, P. Petitjean, B.P. Roques, D. Gerard, E. Stoylova, C. Vuilleumier, S.P. Stoylov, Y. Mely, Properties and growth mechanism of the ordered aggregation of a model RNA by the HIV-1 nucleocapsid protein: an electron microscopy investigation, Biopolymers 45 (1998) 217–229.
[7] S.P. Stoylov, C. Vuilleumier, E. Stoylova, H. De Rocquigny, B.P. Roques, D. Gerard, Y. Mely, Ordered aggregation of ribonucleic acids by the human immunodeficiency virus type 1 nucleocapsid protein, Biopolymers 41 (1997) 301–312.
[8] H. Beltz, C. Clauss, E. Piemont, D. Ficheux, R.J. Gorelick, B. Roques, C. Gabus, J.L. Darlix, H. de Rocquigny, Y. Mely, Structural determinants of HIV-1 nucleocapsid protein for cTAR DNA binding and destabilization, and correlation with inhibition of self-primed DNA synthesis, J. Mol. Biol. 348 (2005) 1113–1126.
[9] J. Godet, N. Ramalanjaona, K.K. Sharma, L. Richert, H. de Rocquigny, J.L. Darlix, G. Duportail, Y. Mely, Specific implications of the HIV-1 nucleocapsid zinc fingers in the annealing of the primer binding site complementary sequences during the obligatory plus strand transfer, Nucleic Acids Res. 39 (2011) 6633–6645.
[10] M.R. Hargittai, R.J. Gorelick, I. Rouzina, K. Musier-Forsyth, Mechanistic insights into the kinetics of HIV-1 nucleocapsid protein-facilitated tRNA annealing to the primer binding site, J. Mol. Biol. 337 (2004) 951–968.
[11] H. Wu, M. Mitra, M.J. McCauley, J.A. Thomas, I. Rouzina, K. Musier-Forsyth, M.C. Williams, R.J. Gorelick, Aromatic residue mutations reveal direct correlation between HIV-1 nucleocapsid protein's nucleic acid chaperone activity and retroviral replication, Virus Res. 171 (2013) 263–277.
[12] H. Beltz, J. Azoulay, S. Bernacchi, J.P. Clamme, D. Ficheux, B. Roques, J.L. Darlix, Y. Mely, Impact of the terminal bulges of HIV-1 cTAR DNA on its stability and the destabilizing activity of the nucleocapsid protein NCp7, J. Mol. Biol. 328 (2003) 95–108.
[13] H. Beltz, E. Piemont, E. Schaub, D. Ficheux, B. Roques, J.L. Darlix, Y. Mely, Role of the structure of the top half of HIV-1 cTAR DNA on the nucleic acid destabilizing activity of the nucleocapsid protein NCp7, J. Mol. Biol. 338 (2004) 711–723.
[14] S. Bernacchi, S. Stoylov, E. Piemont, D. Ficheux, B.P. Roques, J.L. Darlix, Y. Mely, HIV-1 nucleocapsid protein activates transient melting of least stable parts of the secondary structure of TAR and its complementary sequence, J. Mol. Biol. 317 (2002) 385–399.
[15] K.M. Stewart-Maynard, M. Cruceanu, F. Wang, M.N. Vo, R.J. Gorelick, M.C. Williams, I. Rouzina, K. Musier-Forsyth, Retroviral nucleocapsid proteins display nonequivalent levels of nucleic acid chaperone activity, J. Virol. 82 (2008) 10129–10142.
[16] D.F. Qualley, K.M. Stewart-Maynard, F. Wang, M. Mitra, R.J. Gorelick, I. Rouzina, M.C. Williams, K. Musier-Forsyth, C-terminal domain modulates the nucleic acid chaperone activity of human T-cell leukemia virus type 1 nucleocapsid protein via an electrostatic mechanism, J. Biol. Chem. 285 (2010) 295–307.
[17] Q. Darugar, H. Kim, R.J. Gorelick, C. Landes, Human T-cell lymphotropic virus type 1 nucleocapsid protein-induced structural changes in transactivation response DNA hairpin measured by single-molecule fluorescence resonance energy transfer, J. Virol. 82 (2008) 12164–12171.
[18] H. Wu, W. Wang, N. Naiyer, E. Fichtenbaum, D.F. Qualley, M.J. McCauley, R.J. Gorelick, I. Rouzina, K. Musier-Forsyth, M.C. Williams, Single aromatic residue location alters nucleic acid binding and chaperone function of FIV nucleocapsid protein, Virus Res. 193 (2014) 39–51.
[19] D.R. Morcock, S. Katakam, B.P. Kane, J.R. Casas-Finet, Fluorescence and nucleic acid binding properties of bovine leukemia virus nucleocapsid protein, Biophys. Chem. 97 (2002) 203–212.
[20] D.R. Morcock, B.P. Kane, J.R. Casas-Finet, Fluorescence and nucleic acid binding properties of the human T-cell leukemia virus-type 1 nucleocapsid protein, Biochim. Biophys. Acta 1481 (2000) 381–394.
[21] Y. Aida, H. Murakami, M. Takahashi, S.N. Takeshima, Mechanisms of pathogenesis induced by bovine leukemia virus as a model for human T-cell leukemia virus, Front. Microbiol. 4 (2013) 328.
[22] N. Gillet, A. Florins, M. Boxus, C. Burteau, A. Nigro, F. Vandermeers, H. Balon, A.B. Bouzar, J. Defoiche, A. Burny, M. Reichert, R. Kettmann, L. Willems,

Mechanisms of leukemogenesis induced by bovine leukemia virus: prospects for novel anti-retroviral therapies in human, Retrovirology 4 (2007) 18.
[23] G. Gutierrez, S.M. Rodriguez, A. de Brogniez, N. Gillet, R. Golime, A. Burny, J.P. Jaworski, I. Alvarez, L. Vagnoni, K. Trono, L. Willems, Vaccination against delta-retroviruses: the bovine leukemia virus paradigm, Viruses 6 (2014) 2416–2427.
[24] L. Willems, A. Burny, D. Collete, O. Dangoisse, F. Dequiedt, J.S. Gatot, P. Kerkhofs, L. Lefebvre, C. Merezak, T. Peremans, D. Portetelle, J.C. Twizere, R. Kettmann, Genetic determinants of bovine leukemia virus pathogenesis, AIDS Res. Hum. Retroviruses 16 (2000) 1787–1795.
[25] National Animal Health Monitoring System, Bovine Leukosis Virus (BLV) on U.S. Dairy Operations, 2007, USDA-APHIS-VS-CEAH, Fort Collins, CO, 2008.
[26] S.L. Ott, R. Johnson, S.J. Wells, Association between bovine-leukosis virus seroprevalence and herd-level productivity on US dairy farms, Prev. Vet. Med. 61 (2003) 249–262.
[27] G.C. Buehring, S.M. Philpott, K.Y. Choi, Humans have antibodies reactive with bovine leukemia virus, AIDS Res. Hum. Retroviruses 19 (2003) 1105–1113.
[28] G.C. Buehring, H.M. Shen, H.M. Jensen, K.Y. Choi, D. Sun, G. Nuovo, Bovine leukemia virus DNA in human breast tissue, Emerg. Infect. Dis. 20 (2014) 772–782.
[29] D.F. Qualley, C.M. Lackey, J.P. Paterson, Inositol phosphates compete with nucleic acids for binding to bovine leukemia virus matrix protein: implications for deltaretroviral assembly, Proteins 81 (2013) 1377–1385.
[30] L.M. Mansky, R.M. Wisniewski, The bovine leukemia virus encapsidation signal is composed of RNA secondary structures, J. Virol. 72 (1998) 3196–3204.
[31] H. Wang, K.M. Norris, L.M. Mansky, Involvement of the matrix and nucleocapsid domains of the bovine leukemia virus Gag polyprotein precursor in viral RNA packaging, J. Virol. 77 (2003) 9431–9438.
[32] J.G. Levin, J. Guo, I. Rouzina, K. Musier-Forsyth, Nucleic acid chaperone activity of HIV-1 nucleocapsid protein: critical role in reverse transcription and molecular mechanism, Prog. Nucleic Acid Res. Mol. Biol. 80 (2005) 217–286.
[33] J.D. McGhee, Theoretical calculations of the helix-coil transition of DNA in the presence of large, cooperatively binding ligands, Biopolymers 15 (1976) 1345–1375.
[34] M.N. Vo, G. Barany, I. Rouzina, K. Musier-Forsyth, Mechanistic studies of mini-TAR RNA/DNA annealing in the absence and presence of HIV-1 nucleocapsid protein, J. Mol. Biol. 363 (2006) 244–261.